CrossMark

ORIGINAL PAPER

In situ hydrothermal growth of a zirconium-based porphyrinic metal-organic framework on stainless steel fibers for solid-phase microextraction of nitrated polycyclic aromatic hydrocarbons

Jingkun Li[1] · Yaxi Liu[1] · Hao Su[1] · Y.-L. Elaine Wong[2] · Xiangfeng Chen[1] (ORCID) ·
T.-W. Dominic Chan[2] · Qingfeng Chen[1]

Abstract The authors describe the in-situ hydrothermal growth of a porphyrinic zirconium metal-organic framework (MOF), referred to as PCN-222(Zr), on stainless steel fibers. The PCN-222(Zr) is uniformly deposited on the fiber and displays exceptional thermal and chemical stability. The coated fiber was used for the solid-phase microextraction of nitrated polycyclic aromatic hydrocarbons (NPAHs) in water sample prior to their quantitation by gas chromatography in combination with negative chemical ionization mass spectrometry. Limits of detection (S/N = 3) of 17 selected analytes ranged from 0.10 to 20 ng·L^{-1}. Linear range was from 0.4 to 400 ng·L^{-1}. Intra- and inter-day reproducibility values obtained from a single fiber (six replicates) ranged from 2.2–12.8% and 3.6–12.1%, respectively. Fiber-to-fiber reproducibility for six parallel fibers ranged from 3.3% to 10.3% under the same working conditions. The method was successfully applied to determine NPAHs in environmental water, atmospheric particulate matter (PM2.5), and soil samples. This work demonstrated a prominent prospect of this kinds of stable MOF for applications in extraction techniques.

Jingkun Li and Yaxi Liu contributed equally to this work.

✉ Xiangfeng Chen
xiangfchensdas@163.com

1 Key Laboratory for Applied Technology of Sophisticated Analytical Instruments, Shandong Analysis and Test Centre, Shandong Academy of Sciences, Jinan, Shandong, People's Republic of China

2 Department of Chemistry, SAR, The Chinese University of Hong Kong, Shatin, Hong Kong

Introduction

Solid-phase microextraction (SPME), which was introduced by Pawliszyn et al. [1], is an effective sample pretreatment technique. It combines sampling, extraction, pre-concentration, and sample introduction [2]. SPME features a simple, sensitive, solvent free, affordable, portable, and easy automatization [3]. This technique can also be applied to on-site sampling for solid and flowing fluids [4, 5]. As a solvent-free extraction technique, SPME meets key requirements of green analytical chemistry and is highly sensitive for trace-level analysis of environmental [6, 7], food [8], clinical, and biological samples [9].

One of the key challenges in SPME progress is the development of efficient and highly selective fiber coatings. These kinds of fiber coatings increase analyte distribution coefficient between fiber phase and samples, decrease matrix effects, and thus improve sensitivity of analytical method [10]. Metal–organic framework (MOF)-based coating materials attracted significant interest because of their outstanding adsorption efficiencies and modifiable structural features [11–23]. MOF stability values, including those of thermo-, chemical, and hydrostability, are crucial issues that affect their practical applications in SPME [12]. To maintain high adsorption efficiency in various extraction conditions, MOF coating frameworks should be maintained moisture insensitive and chemical resistant in acidic or basic media. MOFs should also withstand up

to 300 °C without phase transformation and structure collapse for thermo desorption and reutilization.

These requirements limit extensive applications of some MOFs as SPME coating materials in high humid conditions [13–16]. For example, the open-metal site of MOF-199 can absorb water molecules and results in decreased adsorption capability toward some aromatic compounds. For other MOFs, such as MOF-5, water molecule attack results in phase transformation and structure collapse of the framework.

Zr(IV) and porphyrinic-based MOFs are appropriate for this challenge than other MOFs because of their high surface area, intrinsic open frameworks, and high stability [24]. Porous coordination network (PCN)-222 (Zr) is a kind of MOF formed by Zr(IV) and tetrakis(4-carboxyphenyl)porphyrin (TCPP). PCN-222 (Zr) can tolerate damage from water, acids, and base because of the strong coordination between Zr(IV) cation and carboxylic oxygen [25, 26]. Although several MOFs were explored as sorbent materials in solid-phase sorption-based extraction techniques, Zr(IV) and porphyrinic-based MOFs remain to be reported.

In this work, PCN-222 (Zr) was initially hydrothermally grown on stainless steel fibers for SPME. Nitropolycyclic aromatic hydrocarbons (NPAHs) are mainly formed during incomplete combustion of organic matter in ubiquitous environmental pollutants and are carcinogenic to humans [19]. NPAHs were determined at trace level in many environmental samples. Thus, analytical methods with high sensitivity must be developed to monitor NPAH levels. Therefore, NPAHs were selected as target analytes to assess SPME fiber performance. Table S-1 shows structure of target analytes. The method was employed for NPAH detection in atmospheric particulate matter (PM$_{2.5}$), environmental water, and soil samples. This letter describes a novel analytical application of PCN-222 (Zr) as coating sorbent for SPME.

Experimental section

Chemicals and reagents

All reagents were of analytical grade. Zirconium (IV) chloride, benzoic acid, acetic acid TCPP and N, N-diethylformamide (DEF) were obtained from Alfa Aesar Company (Shanghai, China, www.alfachina.cn). Deionized water (>18.2 MΩ•cm) was obtained from a Millipore Milli-Q system (Millipore, Bedford, MA, USA, www.merckmillipore.com) and used to prepare aqueous solutions for SPME experiments. Standard mixtures of target analytes at a concentration of 10 μg mL^{-1} in (1:1, v/v) were purchased from AccuStandard (New Haven, CT, USA, www.accustandard.com). These standards were stored in the dark at 4 °C and were used to prepare working standard solutions. Working standard solutions (5.0 μg mL^{-1} in methanol)

were prepared weekly. Cyclohexane and methanol were purchased from Tedia Company Inc., USA (www.tedia.com).
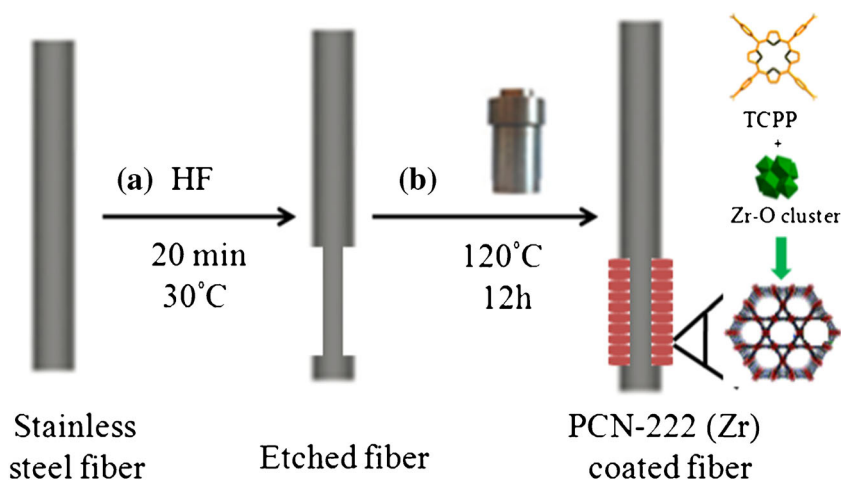
Instrumentation

Stainless steel wire substrate and microliter syringes (10 μL) were purchased from Gaoge Industrial and Trade Co., Ltd. (Shanghai, China). An 85–2 magnetic stirring device and Teflon-coated stir bar (9.9 mm × 5.9 mm × 5 mm) were obtained from Zhongda Instruments Co., Ltd., Jiangsu, China. Quartz filters (1 μm pore size and 88 mm diameter; Pall Gelman Inc., USA) were used for atmospheric particulate matter (PM2.5) collection. An intelligent midvolume suspended particle sampler (Model TH-150A; Wuhan Tian Hong Corporation, China) was used to collect PM$_{2.5}$ samples at 100 L min^{-1} flow rate. Sorbent morphology on SPME fiber was observed by scanning electron microscopy (SEM) (SWPRA™55, Carl Zeiss Micro Imaging Co., Ltd., Germany).Transmission electron microscopy image of powders was observed on a JEOL Ltd. JEM-2100 spectrometer. Thermal gravimetric analysis (TGA) of coated fiber was tested by STA449F3 (Netzsch, Germany) from 50 °C to 500 °C in flowing N$_2$ at a ramping rate of 10 °C min^{-1}. Powder X-ray diffraction (PXRD) pattern was obtained on Bruker Smart Apex CCD-based diffractometer. Brunauer–Emmett–Teller (BET) specific surface areas of typical products were measured using an ASAP 2020 porosimeter (Micromeritics, USA). Agilent gas chromatography (GC) system (7890A, Palo Alto, USA) coupled with negative chemical ionization (NCI) triple quadruple (QqQ) mass spectrometer (7000B, Agilent, USA) was used in all analysis experiments.

Synthesis of MOF

A 10 μL GC microliter syringe and 20 cm stainless-steel wire were used to fabricate the SPME device. First, a naked stainless-steel wire (2.0 cm) was etched with hydrofluoric acid (40%) for 20 min. The coarse surface was washed with methanol and ultrapure water under ultrasonic agitation and air-dried. The etched section of stainless steel wire was immersed in a solution of 25 mg ZrCl$_4$, 10 mg H$_2$TCPP, and 550 mg benzoic acid, and 0.25 mL acetic acid was added in 3 mL DEF in the Teflon linear. The Teflon linear was sealed and placed in steel autoclave at 120 °C for 12 h. MOFs were deposited on fiber. After cooling to room temperature, MOF-coated fiber was removed from the Teflon linear and washed with deionized water and methanol. The fiber was dried at 150 °C for 20 min and then mounted on the microsyringe device for SPME. The fiber was vertically inserted into GC inlet and aged for 1 h at 280 °C.

Fig. 1 Synthesis of PCN-222 (Zr)-based solid-phase microextraction fiber

(a) HF
20 min
30°C

Stainless steel fiber

(b) 120°C
12h

Etched fiber

PCN-222 (Zr) coated fiber

TCPP
+
Zr-O cluster

GC–NCI–mass spectrometry parameters

GC separation was performed using a HP-5MS capillary column with dimensions of 30 m × 0.25 mm and film thickness of 0.25 μm (Agilent Technologies. Inc., USA). Oven temperature was held at 60 °C for 1.0 min and was programmed to increase as follows: at a rate of 15 °C min^{-1} to 150 °C; held for 1 min; at 5 °C min^{-1} to 300 °C; and held for 10.0 min. Helium (99.999%) was used as carrier gas at a flow rate of 1.2 mL min^{-1}. Mass spectrometer was operated in NCI mode.NCI source temperature was selected at 250 °C. Methane 5.5 was used as reagent gas with optimal flow of 40%. Analysis was performed in selective ion monitoring mode.
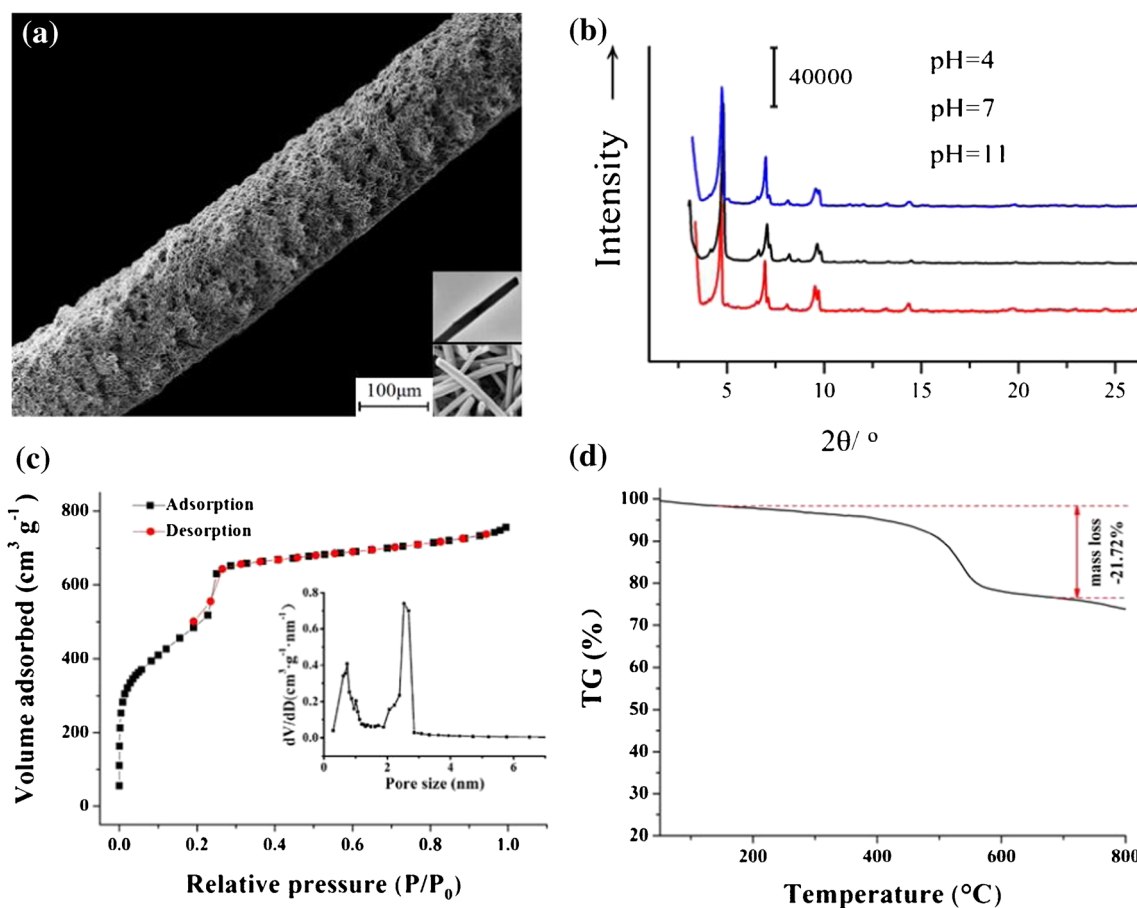

Fig. 2 Scanning electron micrographs of (**a**) PCN-222 (Zr)-coated fiber; (**b**) PXRD spectra of PCN-222 (Zr) peeled from fiber; (**c**) nitrogen adsorption–desorption isotherm of PCN-222 (Zr), inset: pore size distribution; and (**d**) thermogravimetric curve ofPCN-222 (Zr) fibers

Table 1 Enrichment factors (EFs) and selectivity for the selected analytes obtained with the PCN-222 (Zr) SPME fibers

Analyte	EF (mean ± σ)		log K_{ow}
	mode 1[a]	mode 2[b]	
1 N–NAP	321 ± 6.8	983 ± 2.9	2.99
2 N–NAP	341 ± 10.8	941 ± 2.2	6.26
2 N–BiPh	159 ± 4.8	1220 ± 7.0	3.57
3 N–BiPh	103 ± 9.2	1199 ± 7.4	-
5 N–ACE	71 ± 11.2	1873 ± 10.1	7.22
2 N–FLO	<10	1886 ± 6.9	3.83
9 N–ANT	90 ± 8.1	5195 ± 5.4	4.16
9 N–PHE	<10	4195 ± 6.2	4.16
3 N–PHE	<10	2368 ± 7.8	-
2 N–ACE	<10	1100 ± 2.3	-
2 N–FLA	<10	3494 ± 5.4	4.75
3 N–FLA	<10	3519 ± 4.6	4.75
1 N–PYR	<10	3098 ± 9.7	4.75
2 N–PYR	<10	4638 ± 8.0	-
7 N–BaA	<10	5367 ± 13.5	-
6 N–CHR	<10	3093 ± 9.9	5.34
6 N–BaP	<10	2458 ± 5.7	5.93
n-dodecane		31.5	
n-hexane		48.2	
Isooctyl alcohol		5.3	
butanol		1.6	

[a] Headspace mode;

[b] Direct immersion mode;

[c] Not Extracted

SPME procedure

(i) For water samples, water sample (10 mL) was added to a 20 mL glass vial equipped with Teflon-coated magnetic stirrer bar and covered with a cap. Salting out reagent (NaCl) was added before SPME; (ii) for PM$_{2.5}$ and soil samples, target analytes were preliminary extracted using an organic solvent. Collected extract was evaporated, and solvent was substituted by deionized water for SPME. For all samples, direct immersion SPME (DI-SPME) model was used to extract analytes from sample solution. Supplementary information describes detailed sample collection method, extraction procedures, and instrumentation.

Results and discussion

Choice of materials

To date, many MOFs are introduced as coating sorbent for SPME [11–23], which exhibits satisfactory extraction

performance toward pollutants. Among various MOFs, PCN-222 possesses the highest thermo-, chemical, and hydrostability [24]. Despite these properties, as coating materials in SPME, PCN-222 (Zr) remains unreported. Accordingly, a sorbent using PCN-222 (Zr) SPME was developed.

Fig. 1 shows schematic of fabrication of PCN-222 (Zr)-coated SPME fiber. The procedure is a four-step process, which mainly involves hydrothermal growth of MOF on stainless steel fibers. The steps are as follows. Step 1: Metal fiber was etched by hydrofluoric acid and washed with deionized water. Step 2: Etched fiber was immersed in a reagent solution in the Teflon linear for MOF deposition on fiber. Step 3: The MOF-coated fiber was removed from Teflon linear and washed with deionized water and methanol. Step 4: Fiber was mounted carefully into microsyringe device for SPME.

Adsorbent characterization

Fig. 2 (a) shows SEM image of PCN-222 (Zr) coating of SPME fiber. PCN-222 (Zr) crystals deposited on the fiber are rod shaped and approximately 2.4 μm long, in accordance with previous reports [24]. As shown in Fig. 2(b), characteristic diffraction peaks (2.4°, 4.8°, 7.1°, and 9.8°) in PXRD spectrum of powder peeled off from the fiber matched well with simulated XRD patterns, indicating successful crystal synthesis. PXRD patterns of the powder remained intact upon immersion in water and aqueous solutions at pH 4–11 for 10 h, indicating stable MOF and absence of framework collapse or phase transition. N$_2$ adsorption/desorption isotherms are shown in Fig. 2(c). BET surface area of powder measured 2015 m^2 g^{-1}. Inset of Fig. 2(c) shows two types of pores of measuring 1.2 and 3.0 nm; these pores are assigned to triangular and hexagonal meso-channels of the framework. TGA images in Fig. 2(d) show that PCN-222 (Zr)-coated fiber showed minimal weight loss from 50 °C to 400 °C. Pure phase PCN-222 (Zr) grew on the fiber probably because of the initially deposited MOF crystals; these crystals acted as seeds and induced seed-mediated growth [27].

Optimization of extraction conditions

Experimental conditions, including extraction temperature, extraction time, stirring rate, and ionic strength, were optimized to obtain the best extraction performance. Box–Behnken design (BBD) was used to identify optimum extraction parameters through response surface methodology. Fitness and significance of the model were evaluated using ANOVA. Fig. S-1 shows

Table 2 Analytical parameters of PCN-222 (Zr) as SPME sorbent for GC-NCI-MS determination of the selected analytes

Analyte	Linear range (ng L^{-1})	Correlation coefficient (R^2)	LOD (ng L^{-1})	LOQ (ng L^{-1})	Repeatability (RSD%, $n = 6$)	Fiber to fiber reproducibility (RSD%, $n = 3$)
1 N–NAP	2–100	0.9939	0.50	2.00	10.1	7.2
2 N–NAP	2–250	0.9956	0.50	2.00	12.5	5.2
2 N–BiPh	0.4–250	0.9967	0.10	0.40	8.1	12.6
3 N–BiPh	0.4–250	0.9986	0.10	0.40	8.7	4.4
5 N–ACE	4–250	0.9970	1.00	4.00	6.4	4.7
2 N–FLO	4–250	0.9947	1.00	4.00	5.7	2.2
9 N–ANT	2–400	0.9977	0.50	2.00	6.9	9.2
9 N–PHE	4–400	0.9960	1.00	4.00	12.6	5.5
3 N–PHE	1–250	0.9973	1.00	4.00	4.6	3.9
2 N–ACE	5–400	0.9951	2.00	5.00	4.8	13.4
2 N–FLA	10–400	0.9960	5.00	10.0	3.3	5.7
3 N–FLA	25–400	0.9985	10.0	25.0	5.2	4.1
1 N–PYR	25–400	0.9987	10.0	25.0	9.7	9.4
2 N–PYR	50–400	0.9920	20.0	50.0	10.7	14.0
7 N–BaA	2–400	0.9910	0.50	2.00	12.4	11.0
6 N–CHR	10–400	0.9999	5.00	10.0	12.4	12.8
6 N–BaP	50–400	0.9919	20.0	50.0	13.3	11.0

estimated response surface from the BBD for absolute mean responses of analytes obtained by plotting (a) extraction time versus temperature; (b) ionic strength versus temperature; and (c) extraction time versus ionic strength for optimization of extraction step. Extraction time, temperature, and stirring rate were significant model terms because their p-values reached less than <0.001. Optimal extraction conditions were as follows: extraction temperature, 45 °C; extraction time, 60 min; stirring rate, 600 rpm; and ionic strength, 10%.

Analytical figures of merit

Table 1 displays enrichment factors (EFs) of target analytes obtained from spiked water samples. High EFs of NPAHs were obtained for all analytes in DI-SPME model, indicating high affinity of NPAHs toward fiber coating. The open 3D channels conferred PCN-222 with high NPAH storage capacity and benefited SPME enrichment. Fiber selectivity was tested by comparing EFs of n-dodecane, n-hexane, isooctyl alcohol, and butanol along with target analytes in water
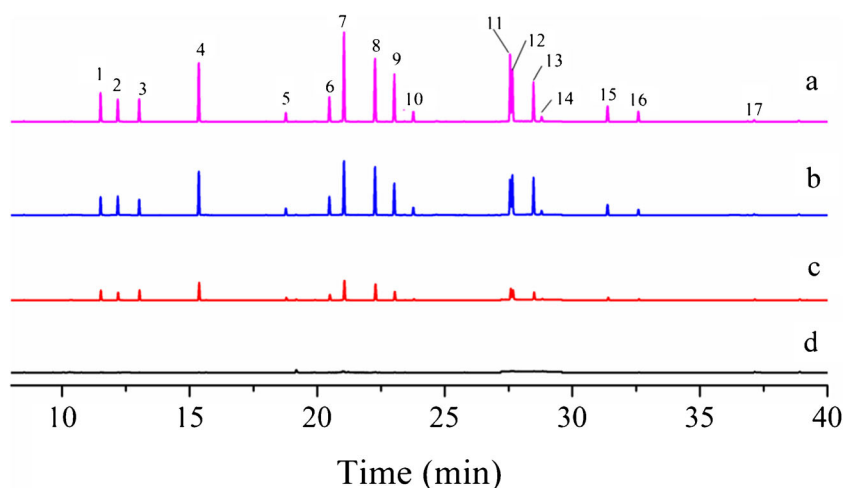
Fig. 3 Typical extracted chromatograms of 17 target analytes of water samples obtained using the method: waste water spiked at (**a**) 0, (**b**) 5, (**c**) 50, and (**d**) 100 ng·L^{-1}. 1: 1-nitronaphthalene; 2: 2-nitronaphthalene; 3: 2-nitrobiphenyl; 4: 3-nitrobiphenyl; 5: 5-nitroacenaphthene; 6: 2-nitrofluorene; 7: 9-nitroanthracene; 8: 9-nitrophenanthrene; 9: 3-nitrophenanthrene; 10: 2-nitroanthracene; 11: 2-nitrofluoranthene; 12: 3-nitrofluoranthene; 13: 1-nitropyrene; 14: 2-nitropyrene; 15: 7-nitrobenzanthracene; 16: 6-nitrochrysene; and 17: 6-nitrobenz(**a**) pyrene

samples. For hydrophilic compounds, including isooctyl alcohol and butanol, almost no enrichment effect was observed using the fiber. EFs of hydrophobic analytes (except *n*-hexane and *n*-hexane) were generally higher than those of hydrophilic analytes. This result indicates that hydrophobicity possibly plays an important role in selectivity. $\log K_{ow}$ of *n*-hexane and *n*-dodecane were higher than that of NNAP, whereas their EFs were lower than that of NNAP. Structurally, the selected alkaline analytes lacked aromatic functional groups. Therefore, they cannot undergo π–π electron stacking interactions with MOF ligands. This performance indicated that existence of π electrons in ligands of sorbents and analytes determines selectivity of PCN-222 (Zr) fiber.

Table 2 shows analytical parameters obtained from spiked water samples using the SPME fiber. Limits of detection (LODs, S/N = 3) and limits of quantification (LOQs, S/N = 10) of 17 selected analytes ranged from 0.10 ng·L^{-1} to 20.0 ng·L^{-1} and from 0.40 ng·L^{-1} to 50.0 ng·L^{-1}, respectively. Linear range reached 0.4 ng·L^{-1} to 400 ng·L^{-1}. Good linearity with correlation coefficients ($r^2 > 0.99$) were obtained from all selected analytes. Sensitivity for NPAHs obtained using the method was higher than those reported using electrochemical methods [25, 26]. As shown in Table S-3, LODs of NPAHs using PCN-222 (Zr) SPME fiber were also lower than that obtained using polydimethylsiloxane (PDMS)/divinylbenzene (DVB) fiber coating, and miniaturized solvent extraction methods [28–37]. The EFs of NPAHs obtained using PCN-222 fiber are generally higher than those of PDMS, carboxen (CAR)/PDMS, and DVB/CAR/PDMS fibers (Fig. S-2). Intra- and inter-day reproducibility values using a single fiber (six replicates) ranged from 2.2%–12.8% and 3.6%–12.1%, respectively. Under the same working conditions, fiber-to-fiber reproducibility for six parallel fibers ranged from 3.3% to 10.3%. In addition, the fiber can be reused over 80 times in water samples.

Analysis of environmental samples

The method was applied to the determination of selected nitrated analytes in environmental water, PM$_{2.5}$, and soil samples. As shown in Table S-4, recoveries of target analytes obtained from spiked drinking samples ranged from 81.2% to 113%. Fig. 3 presents extracted ion chromatogram of 17 analytes from water samples. Nitrated analytes, including NNAP, NBIPH, NNAT, NFLUA, and NFLUA, were detected in waste water samples. Detected NPAHs possibly originated from the wet precipitation around steel mills [38]. Four PM$_{2.5}$ and two soil samples were further used to test the method. NPAH recovery values from spiked PM$_{2.5}$ filter and soil samples ranged from 71.2% to 109.7% (Tables S-5 and 6). As shown in Table S-7, 9 N–ANT is the most dominant NPAHs among samples. For PM$_{2.5}$ samples collected from Taian, concentrations of low-ring NPAHs are high at daytime, similar to that of high-ring NPAHs at nighttime. This phenomenon was

possibly caused by enhanced atmospheric stability in near-surface layer that facilitated pollutant accumulation during nighttime [39]. For PM$_{2.5}$ samples collected from Jinan, total concentration of selected analytes is higher than those from Taian. This result may be due to the heavy vehicle exhaust in the city. This city is also surrounded by mountains on three sides, which disfavor aerosol diffusion [40]. Only several low ring NPAHs were detected in soil samples. Concentrations of selected analytes in topsoil samples were higher than those from subsurface soil. These results demonstrated that the method is applicable for NPAH analysis in environmental samples.

Conclusion

In summary, PCN-222 (Zr)-based SPME fibers were successfully fabricated using in situ growth method. Benefiting from unique adsorption and stability, these fibers were first applied to enrich NPAHs from water, soil, and atmospheric particulate matter samples. High EFs, high sensitivity, and good reproducibility of the analytical method highlight significance of PCN-222 (Zr) in SPME; such properties endow the material with significant applicability potentials for environmental sample treatment. Although MOF-based SPME fibers exhibit excellent extraction performance, bulk production of fibers with uniform coating remains a challenge and needs further investigation.

References

1. Arthur CL, Pawliszyn J (1990) Solid phase microextraction with thermal desorption using fused silica optical fibers. Anal Chem 62: 2145–2148
2. Spietelun A, Kloskowshi A, Chrzanowski W, Namiesnik J (2013) Understanding solid-phase microextraction: key factors influencing the extraction process and trends in improving the technique. Chem Rev 113:1667–1685
3. Li J, Wang YB, Li KY, Cao YQ, Wu S, Wu L (2015) Advances in different configurations of solid-phase microextraction and their applications in food and environmental analysis. Trends Anal Chem 72:141–152
4. Kenessov B, Koziel JA, Orazbayeva D (2016) Perspectives and challenges of on-site quantification of organic pollutants in soils using solid-phase microextraction. Trends Anal Chem 85:111–122
5. Souza-Silva EA, Jiangb R, Rodríguez-Lafuentec A, Gionfriddo E, Pawliszyn J (2015) A critical review of the state of the art of solid-

phase microextraction of complex matrices I. Environmental analysis. Trends Anal Chem 71:224–235

6. Piri-Moghadam H, Ahmadi F, Pawliszyn J (2016) A critical review of solid phase microextraction for analysis of water samples. Trends Anal Chem 85:133–143

7. Souza-Silva EA, Gionfriddo E, Pawliszyn J (2015) A critical review of the state of the art of solid-phase microextraction of complex matrices II. Food analysis. Trends Anal Chem 71:236–248

8. Souza-Silva EA, Reyes-Garcésa N, Gómez-Ríosa GA, Boyaci E, Bojko B, Pawliszyn J (2015) A critical review of the state of the art of solid-phase microextraction of complex matrices III. Bioanalytical and clinical applications. Trends Anal Chem 71: 249–264

9. Spietelun A, Kloskowski A, Chrzanowski W, Namiesnik J (2013) Understanding solid-phase microextraction: key factors influencing the extraction process and trends in improving the technique. Chem Rev 113:1667–1685

10. Silva EAS, Risticevic S, Pawliszyn J (2013) Recent trends in SPME concerning sorbent materials, configurations and in vivo applications. Trends Anal Chem 43:24–36

11. Furukawa H, Cordova KE, O'Keeffe M, Yaghi OM (2013) The chemistry and applications of metal-organic frameworks. Science 341:123044-1–12304412

12. Gu ZY, Yang CX, Chang N, Yan XP (2012) Metal–organic frameworks for analytical chemistry: From sample collection to chromatographic separation. Acc Chem Res 45:734–745

13. Zhang Z, Huang Y, Ding W, Li G (2014) Multilayer interparticle linking hybrid MOF-199 for noninvasive enrichment and analysis of plant hormone ethylene. Anal Chem 86:3533–3540

14. Li H, Shi W, Zhao K, Li H, Bing Y, Cheng P (2012) Enhanced hydrostability in Ni-Doped mOF-5. Inorg Chem 51:9200–9207

15. Shang HB, Yang CX, Yan XP (2014) Metal–organic framework UiO-66 coated stainless steel fiber for solid-phase microextraction of phenols in water samples. J Chromatogr A 1357:165–171

16. Wu YY, Yang CX, Yan XP (2014) Fabrication of metal–organic framework MIL-88B films on stainless steel fibers for solid-phase microextraction of polychlorinated biphenyls. J Chromatogr A 1334:1–8

17. Castillo JM, Vlugt TJH, Calero SJ (2008) Understanding water adsorption in CuBTC metal organic frameworks. Phys Chem C 112:15934–15939

18. Supronowicz B, Mavrandonakis A, Heine T (2013) Interaction of biologically important organic molecules with the unsaturated copper centers of the HKUST-1 metal–organic framework: an ab-initio study. J Phys Chem C 117:14570–14578

19. Cui XY, Gu ZY, Jiang DQ, Li Y, Wang HF, Yan XP (2009) In situ hydrothermal growth of metal−organic framework 199 films on stainless steel fibers for solid-phase microextraction of gaseous benzene homologues. Anal Chem 81:9771–9777

20. He CT, Tian JY, Liu SY, Ouyang G, Zhang JP, Chen XM (2013) A porous coordination framework for highly sensitive and selective solid-phase microextraction of non-polar volatile organic compounds. Chem Sci 4:351–356

21. Li YA, Yang F, Liu ZC, Liu QK, Dong YB (2014) porous Cd(II)-MOF-coated quartz fiber for solid-phase microextraction of BTEX. J Mater Chem A 2:13868–13872

22. Chang N, Gu ZY, Wang HF, Yan XP (2011) Metal–organic-framework-based tandem molecular sieves as a dual platform for selective microextraction and high-resolution gas chromatographic separation of n-alkanes in complex matrixes. Anal Chem 83:7094–7101

23. Yu LQ, Yan XP (2013) Covalent bonding of zeolitic imidazolate framework-90 to functionalized silica fibers for solid-phase microextraction Chem. Commun 49:2142–2144

24. Feng D, Gu ZY, Li JR, Jiang HL, Wei Z, Zhou HC (2012) Zirconium-metalloporphyrin PCN-222: mesoporous metal–organic frameworks with ultrahigh stability as biomimetic catalysts. Angew Chem Int Ed 51:10307–10310

25. Xu HQ, Wang K, Ding M, Feng D, Jiang HL, Zhou HC (2016) Seed-mediated synthesis of metal–organic frameworks. J Am Chem Soc 138:5316–5320

26. Zhang GY, Zhuang YH, Shan D, Su GF, Cosnier S, Zhang XJ (2016) Zirconium-based porphyrinic metal–organic framework (PCN-222): Enhanced photoelectro chemical response and its application for label-free phosphoprotein detection. Anal Chem 88: 11207–11212

27. Jiang HL, Feng D, Wang K, Gu ZY, Wei Z, Chen YP, Zhou HC (2013) An exceptionally stable, porphyrinic Zr metal–organic framework exhibiting pH-dependent fluorescence. J Am Chem Soc 135:13934–13938

28. Barek J, Pumera M, Muck A, Kaderabkova M, Zima J (1999) Polarographic and voltammetric determination of selected nitrated polycyclic aromatic hydrocarbons. Anal Chim Acta 393:141–146

29. Peckova K, Barek J, Moreira JC, Zima J (2005) Polarographic and voltammetric determination of trace amounts of 2-nitronaphthalene. Anal Bioanal Chem 381:520–525

30. Mekiki D, Kalogerakis N, Psillakis E (2006) Application of solid-phase microextraction for the analysis of nitropolycyclic aromatic hydrocarbons in Water. Chromatographia 63:85–89

31. Santos AS, Regis ACD, Rocha GD, Bezerra MA, Jesus RM, Andrade JB (2016) A simple, comprehensive, and miniaturized solvent extraction method for determination of particulate-phase polycyclic aromatic compounds in air. J Chromatogr A 1435:6–17

32. Hung CH, Ho HP, Lin MT, Chen CY, Shu YY, Lee MR (2012) Purge-assisted headspace solid-phase microextraction combined with gas chromatography/mass spectrometry for the determination of trace nitrated polycyclic aromatic hydrocarbons in aqueous samples. J Chromatogr A 1265:1–6

33. Toledo M, Lanças FM, Carrilho E (2007) Solid-phase extraction of nitro-PAH from aquatic samples and its separation by reverse-Phase capillary liquid chromatography. J Braz Chem Soc 18:1004–1010

34. Qiao M, Qi WX, Liu HJ, Qu JH (2014) Oxygenated, nitrated, methyl and parent polycyclic aromatic hydrocarbons in rivers of Haihe River System, China: Occurrence, possible formation, and source and fate in a water-shortage area. Sci Total Environ 481: 178–185

35. Santos LO, Anjos JP, Ferreira SLC, Andrade JB (2017) Simultaneous determination of PAHS, nitro-PAHS and quinones in surface and ground water samples using SDME/GC-MS. Microchem J 133:431–440

36. Guiñez M, Martinez LD, Fernandez L, Cerutti S (2017) Dispersive liquid–liquid microextraction based on solidification of floating organic drop and fluorescence detection for the determination of nitrated polycyclic aromatic hydrocarbons in aqueous samples. Microchem J 131:1–8

37. Chondo Y, Li Y, Makino F, Tang N, Toriba A, Kameda T, Hayakawa K (2013) Determination of selected nitropolycyclic aromatic hydrocarbons in water samples. Chem. Pharm. Bull 61: 1269–1274

38. Jurado E, Jaward F, Lohmann R, Jones KC, Simo R, Dachs J (2005) Wet deposition of persistent organic pollutants to the global oceans. Environ. Sci. Technol 39:2426–2435

39. Tham YWF, Takeda K, Sakugawa H (2008) Polycyclic aromatic hydrocarbons (PAHs) associated with atmospheric particles in Higashi Hiroshima, Japan: Influence of meteorological conditions and seasonal variations. Atmos Res 88:224–233

40. Sun Y, Zhou X, Wai K, Yuan Q, Xu Z, Zhou S, Qi Q, Wang W (2013) Simultaneous measurement of particulate and gaseous pollutants in an urban city in North China Plain during the heating period: Implication of source contribution. Atmos Res 134:24–34